Numerical investigation of ultimate axial capacity of eccentrically loaded steel angles

Iftesham Bashar[1] and Khan Mahmud Amanat[2]

[1]*Department of Civil Engineering*
University of Information Technology and Sciences, Dhaka, Bangladesh
[2]*Department of Civil Engineering*
Bangladesh University of Engineering and Technology, Dhaka, Bangladesh

Abstract

Angles are one of the most common sections used in steel structures. Sometimes an entire structure is composed of steel angle sections such as lattice towers used in telecommunication and power transmission sectors. A lattice tower is generally analyzed and designed assuming that each member is a two-force member subjected to tension and compression only. But in practical cases, single angle members are subjected to axial compression with end moments due to the eccentric connection. Eccentrically loaded single-angle sections are among the most difficult structural members to properly analyze and design. Present study investigates the ultimate compressive load carrying capacity of single steel angles subjected to eccentrically applied axial load as part of a three dimensional truss. In this paper, a previously conducted experimental study is simulated. A finite element study is conducted to properly understand the complex load carrying behavior of single angles. Account is taken of member eccentricity, local deformation as well as geometric and material non-linearity. Results are then compared with previous experimental records. It has been demonstrated that the finite element model predicted the experimental ultimate loads and the behavior of steel angles with reasonable accuracy.

1. Introduction

Steel angles are one of the most common structural member. These are extensively used as primary leg and diagonal members of latticed electrical transmission line towers and antenna-supporting towers; as the chord members in plane trusses; as web and bracing members; open-web steel joists and frames; as lintels spanning openings over doors, windows etc. Such structures are analyzed and designed assuming that each member is a two-force member

subjected to tension and compression only. But in practical cases, in such a structure, the single angle members are connected by one leg to the adjacent members. The resulting eccentricity due to this connection arrangement introduces end moments which are most troublesome to analyze and design when combined with axial compression. Such loading complicates the buckling behavior and creates difficulty in finding a suitable design model. For this reason, eccentrically loaded single-angle structures are among the most difficult structural members to analyze and design. Stang and Strickenberg (1922) conducted the first compression tests on angle members in USA. It was found that load eccentricity and end restraint are very important in evaluating single-angle strength, with load eccentricity having more effect than end restraint for slenderness ratios below about 85. Wakabayashi and Nonaka (1965) studied equal-leg angles under concentric loading for slenderness ratios ranging between 40 and 150. Majority of the specimens failed in flexural buckling and the results obtained were used to develop a design method. Yokoo *et al*. (1968) performed a study of hot-rolled single-angle members loaded concentrically in compression using a ball-joint connection, where torsional deformations were found to be predominant. A buckling mode involving buckling perpendicular to the plane of the connected leg with little twisting up to the maximum load was observed by Trahair, Usami and Galambos (1969) when using fixed or hinged conditions allowing out-of-plane rotations. Kennedy and Murty (1972) presented a rational buckling analysis that was designed to overcome limitations in the American Institute of Steel Construction (AISC) Specifications and the Canadian Standards Association (CSA) design code. Mueller and Erzurumlu (1983) investigated the overall performance of single-angle columns involving parameters: yield stress, load eccentricity, and end restraint. Mueller and Wagner (1983) performed further testing to gain more knowledge regarding the post buckling performance of angle members. Bathon and Mueller (1993) tested a wide range of eccentrically loaded angles using a ball joint to model end conditions unrestrained against rotation. The measured ultimate strengths were compared with the American design code. Experiments were carried out by Adluri and Madugula (1996) on single angles of different cross sectional dimensions and of different slenderness ratios. All the test specimens including those prone to local buckling failed in flexural buckling before exhibiting some local failure. Finally several column curves were developed by Adluri and Madugula (1996) to verify the test results. It was observed that the generated column curves were very close to test results.

Adluri (1994) used Finite Element Method to simulate the behavior of steel angles under flexural buckling. The results show good agreement between theory and experiments. But, A combination of finite element and finite segment approaches has been used by Hu and Lu (1981) to determine the complete load-deflection relationships of single-angle struts subjected to eccentric compressive loads, with or without end restraints. A rational design procedure for eccentrically loaded single angles was also being developed. Liu and Hui (2010) investigated the response of steel single angles subjected to axial eccentric loading by means of finite element method. The results show that for major axis bending, a critical eccentricity exists, below which reduction in ultimate load capacity is marginal. On the contrary, for minor axis bending, the reduction in ultimate capacity due to increase of eccentricity is more significant.
It can be observed from the above-mentioned researches that most of the works related to the investigation of single steel angles are experiment based. Some work has been performed by means of finite element method, but these may not be enough to give a proper correlation between experiment and finite element method. Although angle members are seemingly simple structural shapes used in several kinds of applications, their design is quite complicated and has not been resolved completely to the satisfaction of design engineers. Thus the aim of this paper to investigate ultimate capacity of steel angles eccentrically loaded as part of a latticed structure by means of numerical finite element analysis. Three dimensional finite element studies have been carried out to simulate previously conducted

experimental works by the researchers. Comparison of compressive load capacity of the single angles obtained by finite element analysis and previous experimental results has been made.

2.   Experiment of Elgaaly *et al* (1991)

The paper studies a numerical investigation of the test program carried out by Elgaaly *et al*. In 1991, Elgaaly *et al* conducted tests on 50 non-slender single steel angles as part of a three dimensional latticed truss. Both the specimens with eccentric single bolted and double bolted end connections were investigated. Of the specimens, 25 were double bolted and the rest 22 were single bolted at their ends. Table 1 lists the angle sections by groups depending on difference in cross-sectional dimensions, slenderness ratios (*l/r*) and end conditions. Figure 1 illustrates the test setup of Elgaaly *et al* (1991).

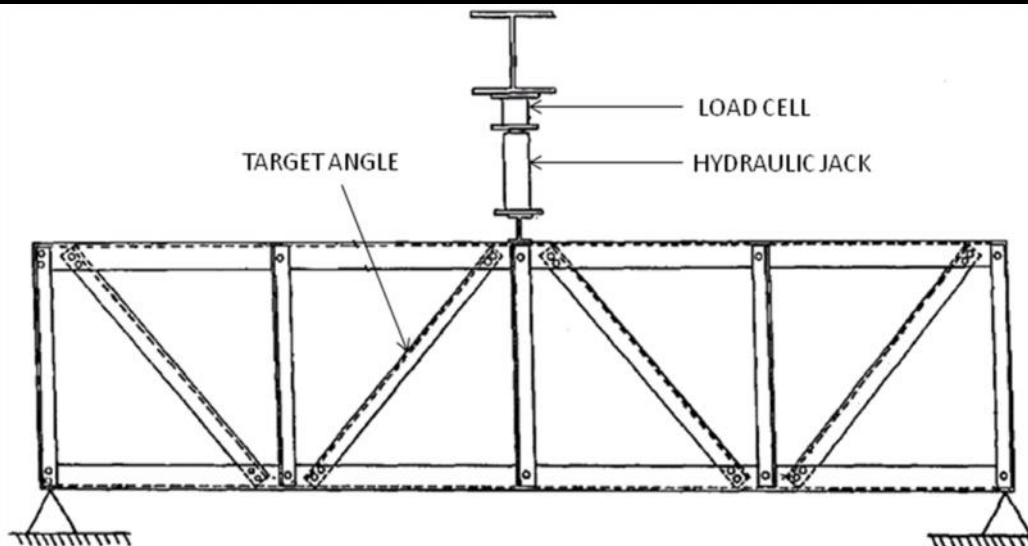| Table 1. Test Specimens				
Group	Size	L / r	End Conditions	Test Nos.
1	1¾ × 1¾ × ⅛	98	double bolt	1, 2, 3, 4, 5
2	1¾ × 1¾ × ³⁄₁₆	99	double bolt	6, 7, 8, 33, 34
3	2 × 2 × ⅛	85	double bolt	9, 10, 11, 12, 13
4	2 × 2 × ³⁄₁₆	86	double bolt	20, 21, 22, 43, 44
5	2½ × 2½ × ³⁄₁₆	87	double bolt	18, 19, 50, 51, 52
6	1¾ × 1¾ × ⅛	92	single bolt	53, 54, 55, 56, 57
7	1¾ × 1¾ × ³⁄₁₆	93	single bolt	23, 24, 35, 36, 37
8	2 × 2 × ⅛	80	single bolt	26, 27, 28, 38, 39
9	2 × 2 × ³⁄₁₆	81	single bolt	29, 31, 40, 41, 42
10	2½ × 2½ × ³⁄₁₆	65	single bolt	45, 46, 47, 48, 49

Fig. 1. General 2-D sketch of test set-up of Elgaaly *et al* (1991)

The selection of specific member sizes for testing was based on both the capacity of the truss and the need to cover slenderness ratio range from 0 to 120. The truss was designed so that the target angle would fail first without introducing significant deformations in the remainder of the truss.
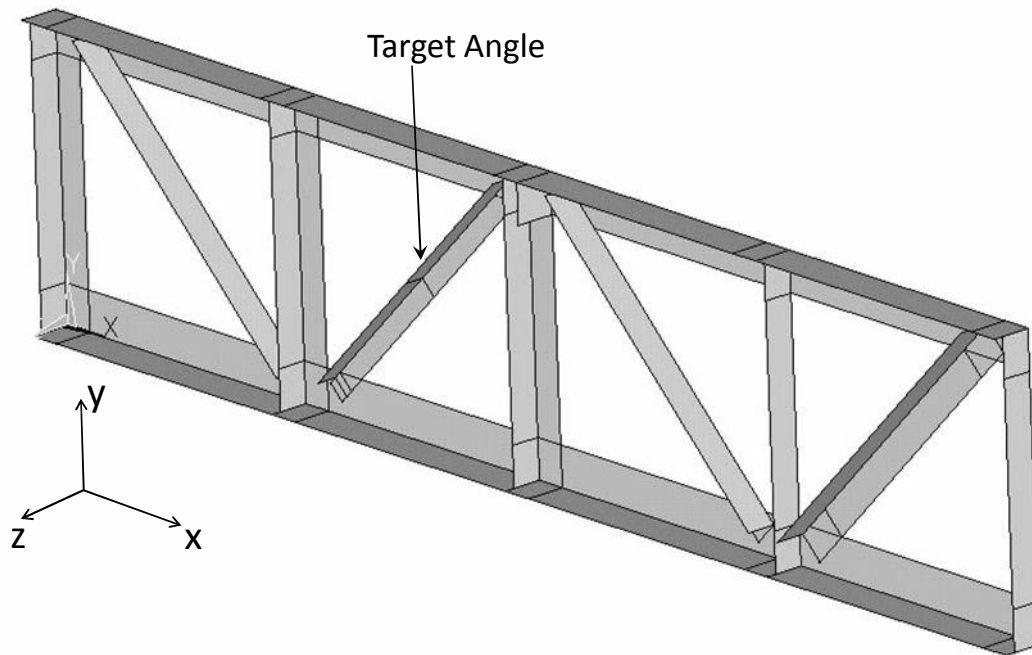
Fig. 2. General 3-D sketch of the truss studied

3.   Computational Modeling

3.1   Finite Element Modeling of the Truss System

Figure 2 shows a general configuration of the three dimensional finite element model of the truss structure. The model consists a target angle as was in the test of Elgaaly *et al* (1991). For the analysis, the entire truss frame has been modeled using finite element package ANSYS. Angle specimens are discretized into a mesh of elements using general-purpose 4-node shell elements.

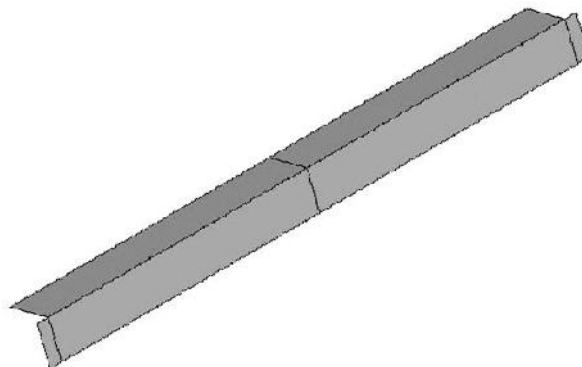### 3.1.1   Meshing of the Angles

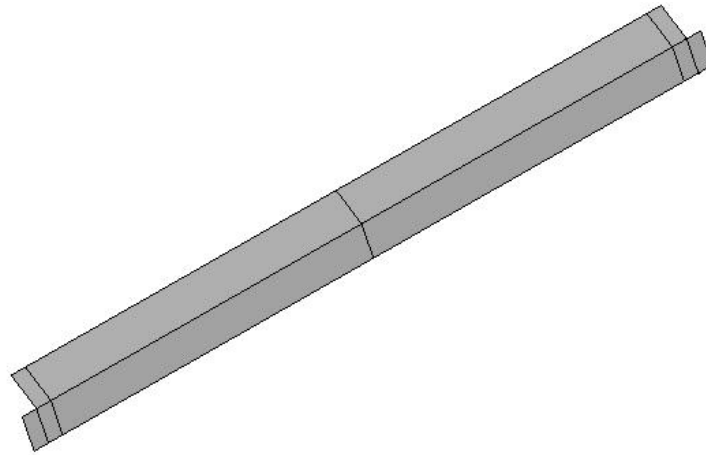Fig. 3. Area formation for meshing of target angle for single bolted specimen

Fig. 4. Area formation for meshing of target angle for double bolted specimen

Each of the single angle members is divided along its width. Individual division is rectangular. In the finite element model of the present study the target angle is discretized into finer mesh sizes (figure 5) considering the cross-sectional dimensions of the target angle rather than the dimensions of other angle members. The meshing of the remaining truss members has been done in such a manner so that the overall mesh size for each member remains uniform and the aspect ratio of the elements is reasonable. Figure 3 and figure 4 illustrate the area formation of target angles for meshing of single and double bolted specimens. And figure 5 shows the junction of the lower portion of double-bolted target angle with bottom chord.
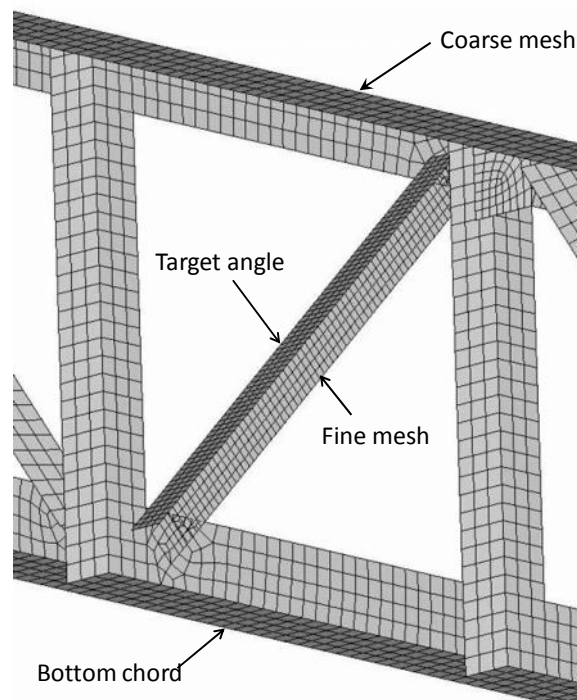

Fig. 5. Close-up view of junction of a double bolted target angle with bottom Chord
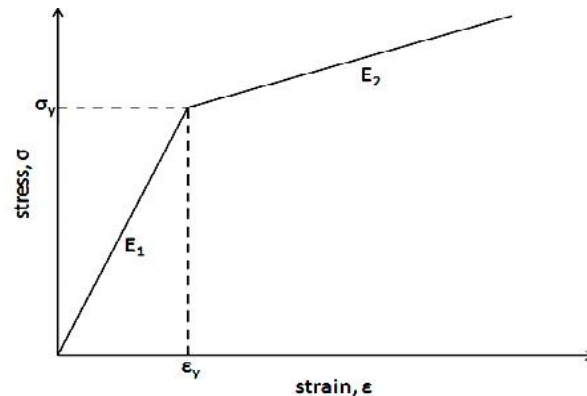
3.1.2   Material Properties

Fig. 6. Bilinear kinematic hardening (BKIN)

The materials for the elements have been taken as bilinear kinematic hardening (BKIN). According to Finite Element Software ANSYS 11.0 Help Menu, the option assumes that the total stress range is equal to twice the yield stress, which is recommended for general small-strain use for materials that obey von Mises yield criteria (which includes most metals).

In the figure 6,

$\dagger_y$ = yield stress
$\vee_y$ = strain corresponding to yield stress
E_1 = modulus of elasticity up to yield point
E_2 = modulus of elasticity after exceeding yield point

The Poisson's ratio is taken as 0.25. The modulus of elasticity of the angle members has been assumed 200 kN/mm^2 (the modulus of elasticity of steel).

3.2   Boundary Conditions

In case of the bottom horizontal truss member, the leftmost node is kept restrained in X and Y-directions (axes notation is mentioned in figure 2). And the corresponding rightmost node is kept restrained in Y and Z- directions. The junction nodes of the leftmost and rightmost vertical angles with bottom horizontal angle are restrained in Y-direction only. Rest of the nodes are kept restrained in Z-direction only to prevent out-of-plane instability of the truss. The boundary conditions for the present study has been revealed in figure 7.
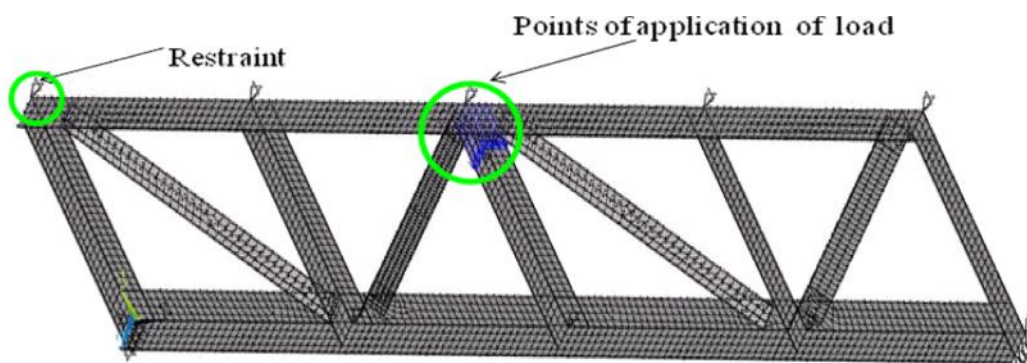

Fig. 7. Finite element model with loads and boundary conditions

3.3   Loads

The load has been applied on the middle vertical angle member at its junction nodes with the top chord to allow the whole structure systematically deform.
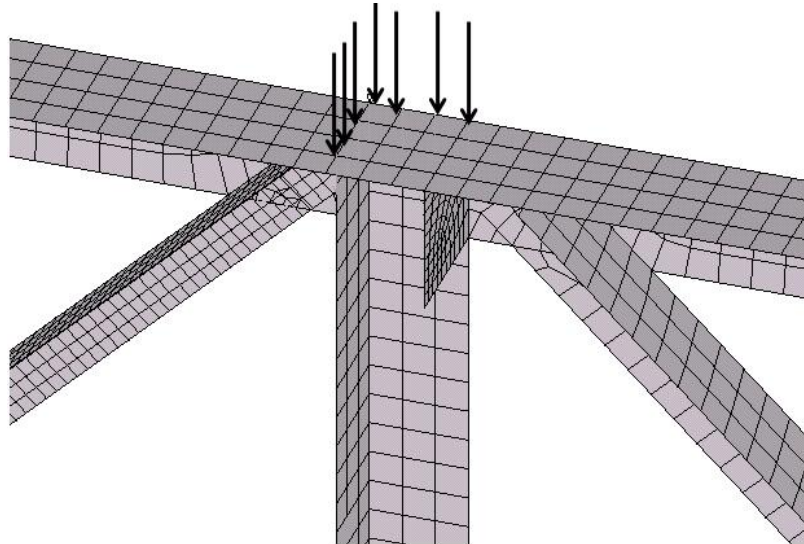

Fig. 8. Close-up mesh with loads and boundary conditions

In the present analysis, the load is applied slightly greater than the Euler Load of the corresponding target angle member for each case. Then the load has been augmented and then subdivided equally into the junction nodes to be applied on the truss structure (figure 8).

3.4   Determination of Member Force of Target Angle

In the present study, the member force of target angles have been calculated using element stresses (elemental stresses have been obtained from non-linear static analysis of the truss). Then using the universal equation:

$$\sum Force = \sum \left[\left(Stress \right) \times \left(Area \right) \right] \tag{1}$$

the member force has been evaluated. For this purpose, at first, the angle member has been divided into two equal divisions (figure 9(a) and figure 9(b)).

(a)   Single bolted angle   (b) Double bolted angle
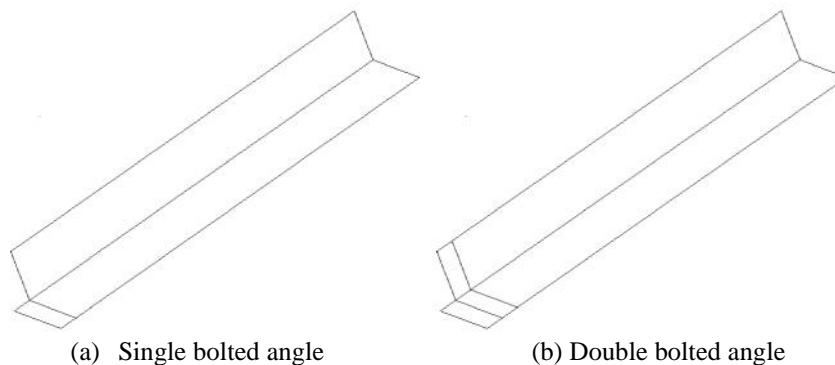
Fig. 9. Area formation of target angle (half of the specimen)

Then, taking either the lower half or the upper half portion, an infinitesimal strip of a number of elements have been chosen as target whose stresses are to be obtained (figure 10(a)). Finally, the member force has been calculated by directly integrating the multiplication of individual element stress and corresponding element area as shown in figure 10(b).

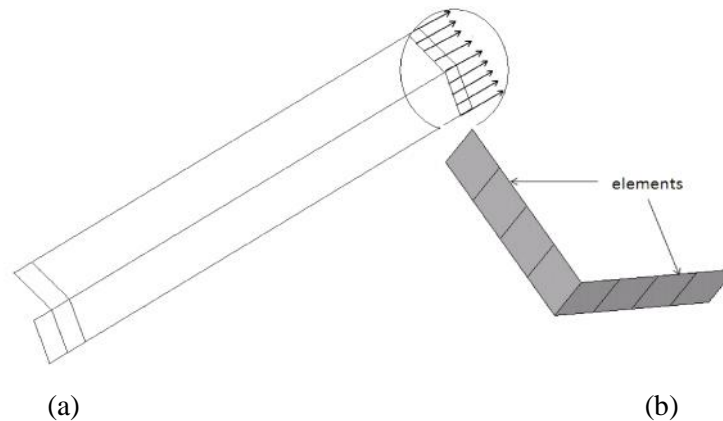(a)   (b)

Fig. 10. (a) Typical element divisions along the mid cross-section of a double bolted target angle for calculating element stresses to obtain the member force of the corresponding angle (b) typical elements (close-up view)

4.   Results and Discussions

4.1   Validation of Finite Element Model

Elgaaly described the member force vs displacement graphs of 2 single bolted (test 42 and test 26) and 2 double bolted (test 34 and test 9) target angles. The same specimens are analyzed by means of finite element method. It has been observed from the comparative figures that results from test of Elgaaly and from present analysis are relatively close for all the specimens except for specimen of test 26 (the reason may be the higher w/t ratio of the specimen, which is 13.88 as mentioned by Elgaaly). Here comparative results for test 34 and test 42 have been represented graphically (figure 11 and figure 12). The observed deviations, though not significant between both present analysis and test results of Elgaaly may be due to the fact that during modeling the truss system, bolted connection is simply replaced by modeling the connecting portions as the integral parts as the component angle members. So in the finite element model considered here, no stress concentration has occurred. So, some minor differences occur for some of the angles.
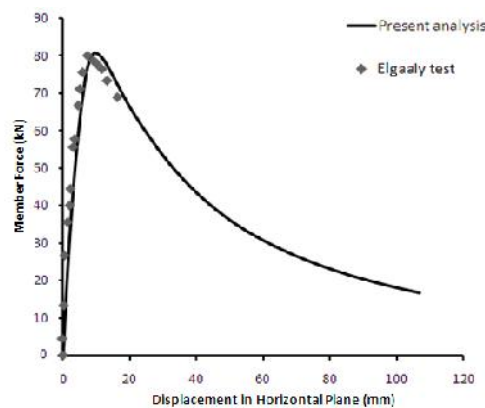

Fig. 11. Load-deflection graph of angle size L 45.57×45.57×5.00, double bolted (test 34)
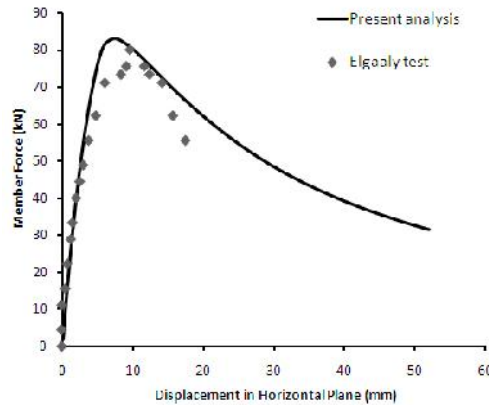
Fig. 12. Load-deflection graph of angle size L 50.75×50.75×4.83, single bolted (test 42)

Overall, finite element analysis gives more logical results for double bolted angles than for single bolted specimens as the prevailing methodology of modeling the truss frame in finite element is more compatible to the restraint conditions of double bolted conditions (more fixity in double bolted than single bolted connections).

4.2   Deformation Characteristics of the Target Angle

The peak load is the indicator which shows that from this point buckling of the structure initiates especially of target angle, as the other truss members except the target angle is designed in such a way so that the buckling starts within the target angle at first and eventually the failure of the target angle occurs without any significant deformation in the rest of the truss. The deformation characteristics can be easily explained by considering the specimen of test 53 of Elgaaly. The specimen is single bolted and has width-thickness ratio is equal to 13.15 with slenderness ratio of 92.0 (the highest ratio of all the groups of single bolted target angles). From finite element analysis the obtained failure load is 47.42 kN whereas compressive load carrying capacity from the test of Elgaaly is 48.04 kN.
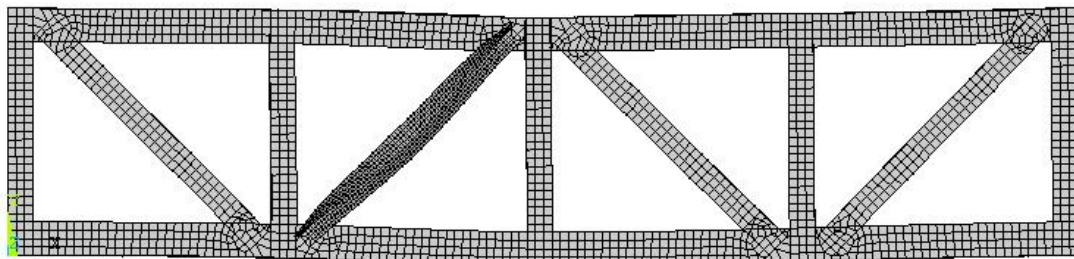

Fig. 13. (a) Deflection pattern at the early stage of buckling (front view)

Fig. 13. (b) Deflection pattern at the early stage of buckling (top view (close-up))

In the initial stage, when the load reaches the pick, no significant deformation is observed initially. But gradually when the load tends to decrease and reaches a small but considerable percentage of the peak load value, some extent of deformation occurs. In this stage, the deflection initiates with the bending of the connected leg of the target angle. The rest of the truss members are in the position where they were initially (figure 13(a) and (b)).

When the load value eventually diminishes and comes to the final diminishing point, the deflection is associated with the bending of the connected leg along with the twisting of the unconnected leg of the target angle. Additionally the unconnected leg of the top horizontal member also faces twisting. The lower middle half portion of the target angle faces severe bending stress specially the lowermost connected region of the target angle.

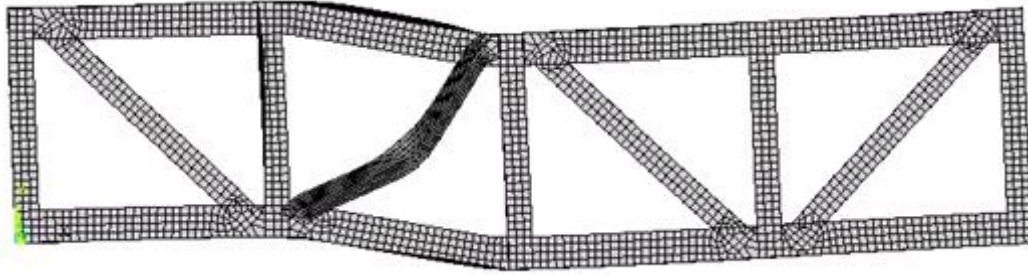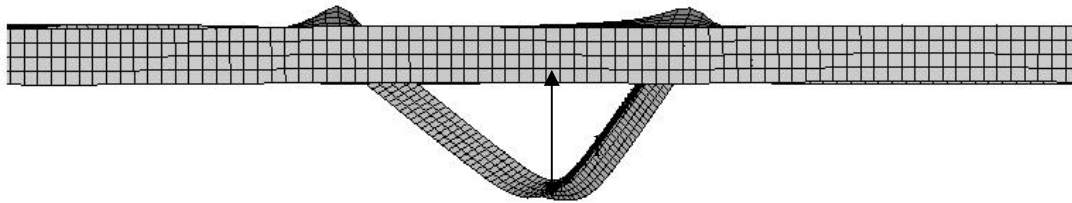Fig. 14. (a) Deflection pattern at the final stage of buckling (front view)

Fig. 14. (b) Deflection pattern at the final stage of buckling (top view (closeup))

The middle vertical angle and the corresponding junction have displaced downwards from their original position. The deflected shapes of the target angle can be easily realized from figure 14(a) and figure 14(b).

4.3 Axial Force vs Lateral Displacement Response

The load-deflection relationship has been signed out as the best characterization of the load carrying behavior of single steel angles subjected to eccentric axial loads. During present analysis of the truss, a load was imposed on the structure sub diving it on each of the junction nodes of the middle vertical angle with the top chord.

Due to the nodal loads, each time target angle has undergone an axial compressive force along with some axial shortening, which is the axial displacement (δ_a) of target angle (shown in figure 15) and at the same time, some lateral displacement (δ_l) occurs (as shown in figure 14(b)). At different stages of applying load, corresponding axial forces and the lateral displacements (δ_l) have been obtained. Typical axial load (P) versus lateral displacement (δ_l) curves obtained for different angle sections from non-linear finite element analysis using this methodology are shown in figures 16 (for single bolted angles)and figure 17 (for double bolted angles), where response is observed to be linear until failure.

In the figure 15,

F = applied load on truss
R = support reactions
P = axial compressive load capacity of the target angle
δ_a = axial displacement (shortening) due to applied compressive load
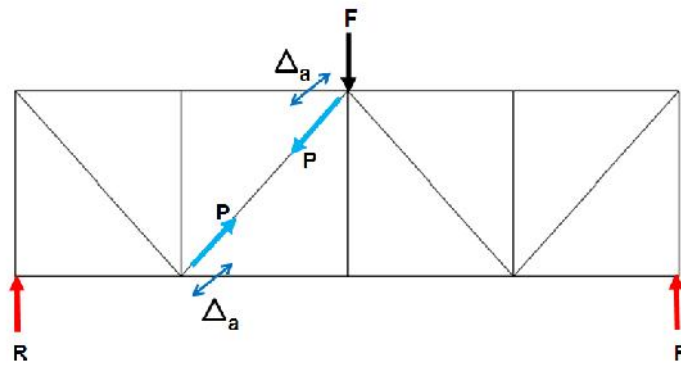
Fig. 15. General two-dimensional figure of the model

Different failure modes with distinguished failure loads have been found for both single bolted and double bolted specimens. For the ease of discussion, 8 specimens (4 single bolted and 4 double bolted) are chosen by the authors as the representative of 47 specimens to describe the salient features of the buckling analysis of the target angles. The single bolted target angles are designated by the test number: 53, 35, 31, and 42 and the double bolted target angles are designated by test number: 1, 34, 20 and 18 according to the test of Elgaaly *at al* (1991). The geometric properties as well as loading conditions etc of the reference specimens aforementioned are listed in the table 2(a) and table 2(b).

Table 2(a)
Properties of Reference Specimens (single bolted)

test no.	width, w (mm)	thickness, t (mm)	w/t	slenderness ratio, l/r	yield stress, F_Y (kN/mm^2)	Failure load (kN)	
						Elgaaly Test	Present Analysis
42	50.75	4.83	10.52	81	317.9	80.51	83
35	44.93	5.13	8.76	93	339.9	75.44	77.71
31	50.39	5.08	9.92	81	339.2	85.98	91.41
53	44.42	3.38	13.15	92	353	48.04	47.42

As expected, all samples failed due to buckling of the connected leg of the target angle. The failure mode was global flexural torsional (FT) mode without local buckling of the angle leg which is similar to the failure mode of specimen 24 as described by Elgaaly *et al* (1991). As observed, all the load-deflection graphs show the same trend. Once the peak load is reached, it eventually diminishes with further increase of deflection.
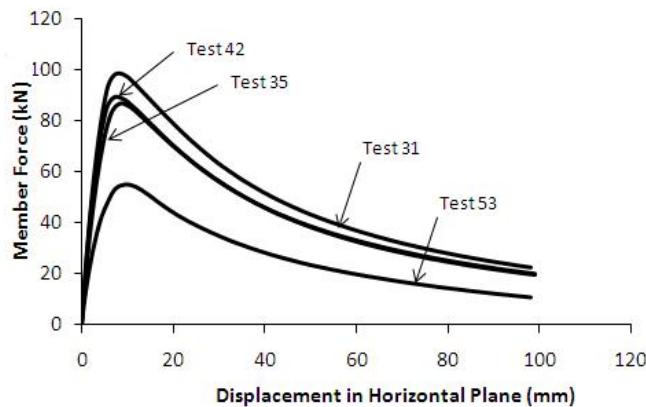

Fig. 16. Typical axial force vs lateral displacement (in horizontal plane) graph for single bolted angles obtained from Present Analysis

Table 2(b)
Properties of Reference Specimens (double bolted)

test no.	width, w (mm)	thickness, t (mm)	w/t	slenderness ratio, l/r	yield stress, F_Y (kN/mm^2)	Failure load (kN)	
						Elgaaly Test	Present Analysis
18	63.17	5.05	12.50	67	315.2	112.7	114.2
20	50.6	5.08	9.96	86	326.9	97.5	92.1
34	45.57	5	9.11	99	342.8	80.2	80.9
1	43.97	3.53	12.45	98	344.1	49.2	53.7

From the illustration of figure 16, different peak loads for the reference specimens have been observed for double bolted angles like single bolted angles. In all cases, with the increase of slenderness ratio, load capacity of angle sections decrease.

Fig. 17. Typical axial force vs lateral displacement (in horizontal plane) graph for double bolted angles obtained from Present Analysis

4.4   Correlation between Test and Present Study

Correlation between test data of Elgaaly *et al* (1991) and present analysis are studied for single and double bolted angles (shown in figure 18 and figure 19 respectively).

Correlation coefficient

Fig. 18. Correlation between failure loads from test of Elgaaly *et al* (1991) and present study for single bolted target angles

$$y = 1.025x - 4.102$$
$$R^2 = 0.879$$

Fig. 19. Correlation between failure loads from test of Elgaaly *et al* (1991) and present study for double bolted target angles
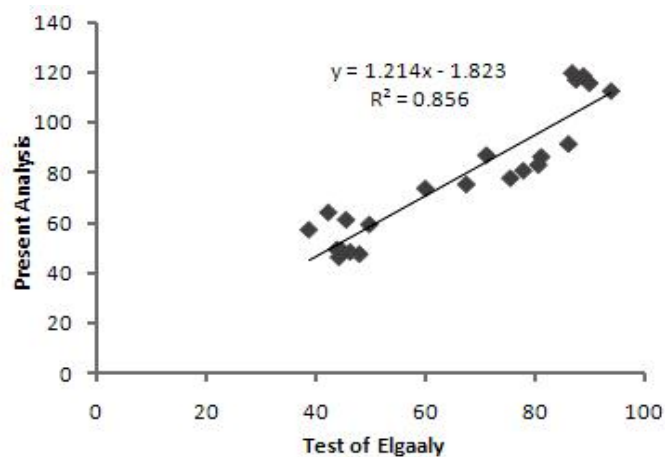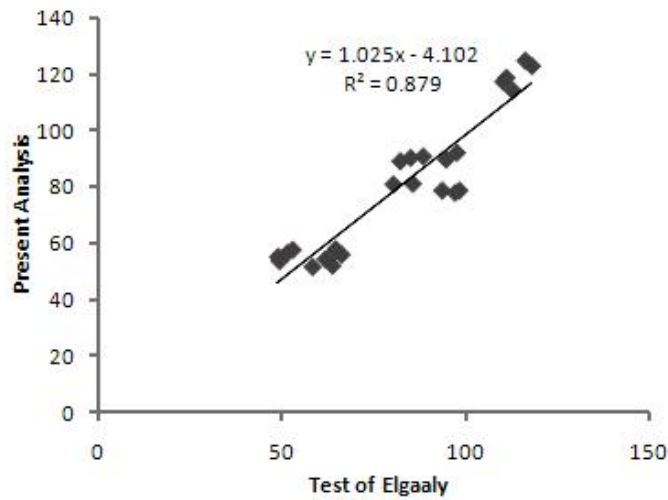
Correlation co-efficient, R= $\sqrt{0.856} = 0.925$ (for single bolted angles)

= 0.938 (for double bolted angles)

Generally, the correlation coefficient, *R*, ranges from -1 to +1. The correlation co-efficients as obtained for both single and double bolted angles indicate that the load capacities from both the test of Elgaaly *et al.* (1991) and present study are fairly close to each other. So, there are very good correlations between the two studies.

4.4.1 Buckling load factor (n)

For better comparison of the buckling loads a parameter called *Buckling load factor (n)* has been calculated similar to study of Elgaaly *et al* (1991). It is defined as the ratio of the failure load divided by the uniform yield capacity of the section (yield stress multiplied by the cross-sectional area), This facilitates the accounting for the effect of the variations in area and yield stress among the test specimens. Moreover % difference in *n* values of both single bolted and double bolted angle specimens have been calculated. Table 3 pairs groups by size and lists the percent difference in *n* values between the corresponding groups. The average *n* values for both single and double bolted target angles have been summarized in figure 20 and figure 21 respectively.
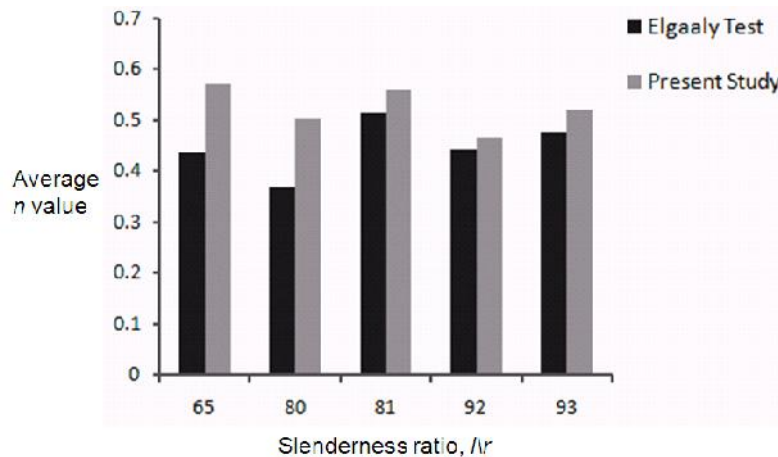

Fig. 20. Comparison of buckling load factor, *n* for different groups of single bolted angles

Table 3
Comparison of single bolted versus double bolted angles

Group (1)	Angle size (2)	*l/r* (3)	End conditions (4)	Elgaaly test		Present analysis	
				Average *n* (5)	Percent difference in *n* (6)	Average *n* (7)	Percent difference in *n* (8)
1	44.45x44.45x3.18	98	Double	0.582	31	0.521	11
6	44.45x44.45x3.18	92	Single	0.444		0.468	
2	44.45x44.45x4.76	99	Double	0.636	34	0.554	6
7	44.45x44.45x4.76	93	Single	0.476		0.522	
3	50.8x50.8x3.18	85	Double	0.525	43	0.530	6
8	50.8x50.8x3.18	80	Single	0.368		0.502	
4	50.8x50.8x4.76	86	Double	0.575	12	0.581	4
9	50.8x50.8x4.76	81	Single	0.514		0.560	
5	63.5x63.5x4.76	67	Double	0.556	27	0.585	2
10	63.5x63.5x4.76	65	Single	0.438		0.572	

From figure 20 and figure 21 as well as in Table 3, it is seen that the double-bolted specimens are stronger than the single-bolted specimens. From test, the average *n* value for the double-bolted specimens is 0.575, which is 28% higher than that of the single-bolted specimens and from finite element analysis, the average *n* value for the double-bolted specimens is 0.554, which is 5.5% higher than that of the single-bolted specimens. Moreover, from finite element analysis, % difference in average *n* values for the double-bolted specimens is 3.79, which is quite reasonable. But, for the single bolted angles, the % difference is 17.14 which is probably significant.

In general, as observed, failure mechanism and load versus displacement characteristics vary depending on *w/t* ratio, end restraints and slenderness ratio.

4.4.2   *Effect of w/t ratio*

It has been observed that in case of single bolted specimens, target angles of group-6, as the width-thickness ratio decreases, the failure load evaluated from finite element analysis increases proportionally. For higher *w/t* ratios, out of plane buckling occurs as in the case of single bolted specimen of test number 53 (according to the test of Elgaaly *et al* (1991)).
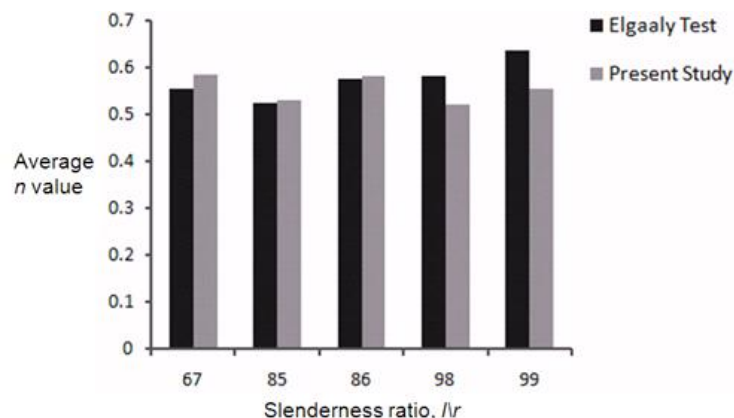

Fig. 21. Comparison of buckling load factor, *n* for different groups of double bolted angle

4.4.3   Effect of end restraints

The difference in strength between the corresponding groups with double and single bolted connections is primarily due to the difference in end restraint conditions. In the test of Elgaaly, the largest difference in *n* values occurs between groups 3 and 8 (43%). On the other hand, from the finite element analysis, the largest difference in *n* values occurs between groups 1 and 6 (11%). This difference is mostly attributed to significantly higher stress concentrations in the single-bolted connections as compared with the double-bolted connections. The smallest difference in strength is between groups 4 and 9 (12%) from test results, whereas, the smallest difference in *n* values occurs between groups 5 and 10 (2%) from finite element study. According to the test results of Elgaaly *et al* (1991), the failure modes for both of these groups are the same, with the dominant effect being global flexural buckling, which tends to emphasize the importance of the difference in rotational end restraint as opposed to local leg crippling.

4.4.4   Effect of slenderness ratio

It is expected that with the increase of slenderness ratio, axial load carrying capacity of single steel angles decrease. But this is the case with a concentrically loaded structure. But in case of eccentrically loaded structures, with the increase of slenderness ratio, failure load does not decrease, rather it increases. This is the case with the test specimens of Elgaaly. Both the test results and the results from finite element analysis exhibit same behavior.

4.4.5   Relationship between Slenderness and Strength

Another area that requires explanation is the difference in failure loads between groups of different sizes and similar end conditions. It is intuitively expected that column strength increases with decreasing *L/r* ratios, and *n* approaches unity as *L/r* approaches a limiting value close to zero. However, this is the case only for concentrically loaded struts, which do not exhibit local failures or torsional effects. All of the specimens tested were loaded eccentrically, and most exhibited significant local and torsional deformations. As a result, *n* does not necessarily increase with decreasing *L/r* values. This is true for both the single and double bolted specimens for the results obtained from test of Elgaaly *et al*. For example, group 2 has an *L/r* ratio of about 99 and double-bolted ends, and group 4 has an *L/r* ratio of 86 and double-bolted ends as well, yet the average *n* value for group 4 is 12% lower than that of group 2. One reason for the difference is the presence of local-torsional effects in group 4 (*b/t* is about 10), which do not occur in group 2 (*b/t* is about 9). Further, since all of the angles were fabricated with the bolt holes centered on the connected legs, the load eccentricity was slightly greater for group 4 (*b* = 2 in.) than for group 2 (*b* = 1.75 in.). This same reasoning applies when comparing any two groups with similar end conditions that indicate decreasing *n* values with decreasing *L/r* values. But, the same groups (group 2 and group 4) exhibit increase of average n value for the decrease of *L/r* ratio observed from finite element analysis. In this case, n value for group 4 is about 4.9% higher than that for group 2. It is of interest to note that groups 7 and 9, which are the single-bolted counterparts of groups 2 and 4, exhibit increasing *n* values with decreasing *L/r* values from test results of Elgaaly as is intuitively expected. This is because the single-bolt connections cause identical flexural-torsional failure in both groups 7 and 9, whereas the predominant failure mode in group 2 is different from that of group 4. Finite element study also shows the same behavior for groups 7 and 9, where n value for group 9 is about 7.3% higher than that for group 7. The average *n* values for angles of all the groups exhibit same behavior as in the test of Elgaaly, except for group 5 and group 10.

5.   Conclusions

The study originated with the aim to validate, through numerical simulation, the eccentric compressive load carrying capacity of a single steel angle (designated as target angle; either single bolted or double bolted) as part of a three-dimensional truss tested by Elgaaly *et al* (1991). The results of present study are in well agreement with those obtained from test of Elgaaly (1991). Therefore, FE analysis may be a good alternative to experiments of single angle structures and can be used for routine design of steel angles which will be helpful to find out better solutions for engineers.

It has been observed that other than slenderness ratio, axial capacity of single angles are dominated by many other factors, such as- the width-thickness ratio, nature of end restraints, eccentricity of applied load etc. The effect of these parameters are required to be included in the design equations for determining ultimate load capacity of single steel angles as part of a three dimensional structure. These findings create further scope of study regarding these parameters on strength of steel angles.

References
Adluri, S. M. R., Studies on Steel Angle Columns, PhD dissertation, Department of Civil and Environmental Engineering, University of Winsor, Winsor Ontario, Canada, 1994.
Adluri, S. M. R., and Madugula, M. K. S., "Development of Column Curve for Steel Angles," Journal of Structural. Engineering, ASCE, Vol. 122, No. 3, P. 309-317, March, 1996.
Ansys 11 Help, "Plastic Material Options Modeling Material Nonlinearities," Nonlinear Structural Analysis, Chapter 8.
Bathon, L., Mueller, W. H., and Kempner, L., "Ultimate Load Capacity of Single Steel Angles," Journal of Structural Engineering, ASCE, Vol. 119, No.1, P. 279-300, Jan., 1993.
Elgaaly, M., Dagher, H., and Davids, W., "Behavior of Single Angle Compression Members," Journal of Structural Engineering, ASCE, Vol.117, No. 12, P. 3720-3741, Dec., 1991.
Hu, Xue-Ren, and Lu, Le-Wu, "Ultimate Strength Analysis of Single Angle Struts with End Restraints," Report No. 471. 3, Firtz Engineering Laboratory, Lehigh University, Bethlehem, Pa., 1981.
Kennedy, J. B., and Murty, Madugula, K. S., "Buckling of Steel Angle and Tee Struts," Journal of the Structural Division, ASCE, Vol. 98, No. ST11, P. 2507-2522, Proc. Paper 9348, Nov., 1972.
Liu, Y., and Hui, L., "Behaviour of Steel Single Angles Subjected to Eccentric Axial Loads," Can. J. Civ. Eng, Vol. 37, No. 6, P. 887-896, 2010.
Mueller, W. H., and Erzurumlu, H., "Limit State Behavior of Steel Angle Columns," Civil-Structural Engineering Division of Engineering and Applied Science, Portland State University, Portland, Oreg, 1983.
Mueller, W. H., and Wagner, A. L., "Plastic Behavior of Steel Angle Columns," Civil-Structural Engineering Division of Engineering and Applied Science, Portland State University, Portland, Oreg, 1983.
Stang, A. H., and Strickenberg, L. R., "Results of Some Compression Tests of Structural Steel Angles," Technologic Paper of the United States Bureau of Standards No. 218, Government Printing Office, Washington, D. C., 1922.
Trahair, N. S., Usami, T., and Galambos. T. V., "Eccentrically Loaded Single Angle Columns," Research Report No. 11, Department of Civil and Environmental Engineering, Washington University. St. Louis, Mo., Aug., 1969.
Wakabayashi, M., and Nonaka, T., "On the Buckling Strength of Angles in Transmission Towers." Bulletin of the Disaster Prevention Research Institute, Kyoto University, Kyoto, Japan, Vol. 15, Part 2, No. 91, P. 1-8, Nov., 1965.
Yokoo, Y., Wakabayashi. M., and Nonaka. T., "An Experimental Study on Buckling of Angles," Yawata Technical Report No. 265, Yawata Iron & Steel Co., Ltd., Tokyo, Japan, P. 8543-8563 and P. 8759-8760, Dec., 1968 (in Japanese).